Journal of Applied Polymer Science

Experimental and computational study of microfluidic flow-focusing generation of gelatin methacrylate hydrogel droplets

Roya Samanipour, Zongjie Wang, Ali Ahmadi, Keekyoung Kim
School of Engineering, University of British Columbia, Kelowna, British Columbia, V1V 1V7, Canada
Correspondence to: K. Kim (E-mail: keekyoung.kim@ubc.ca)

ABSTRACT: This work presents the experimental and computational study of droplet generation for hydrogel prepolymer solution in oil using a flow-focusing device. Effects of different parameters on hydrogel droplet generation and droplet sizes in a flow-focusing device were investigated experimentally and computationally. First, three dimensional (3D) computational simulations were conducted to describe the physics of droplet formation in each regime and mechanism of three different regimes: squeezing, dripping, and jetting regime of hydrogel were investigated. Subsequently, the effects of viscosity, inertia force, and surface tension force on droplet generation, and droplet size were studied through these experiments. The experiments were carried out using different concentration of gelatin methacrylate (GelMA) hydrogel (5 wt % and 8 wt %) as the dispersed phase and two different continuous phase liquids (light mineral oil and hexadecane) with various concentrations of surfactant (0 wt %, 3 wt %, and 20 wt %). All experimental data was summarized by capillary number of dispersed phases and the continuous phases to characterize the different regimes of droplet generation and to predict the transition of dripping to a jetting regime for GelMA solution in flow-focusing devices. It is shown that the transition of dripping to a jetting regime for GelMA happens at lower capillary numbers compared to aqueous solutions. Moreover, by increasing the viscous force of continuous phase or decreasing the interfacial force, the size of GelMA droplets was decreased. By controlling these parameters, the droplet sizes can be controlled between 30 μm and 200 μm, which are very suitable for cell encapsulation. © 2016 Wiley Periodicals, Inc. J. Appl. Polym. Sci. **2016**, *133*, 43701.

KEYWORDS: biomedical applications; hydrophilic polymers; microfluidics; microgels

Received 11 December 2015; accepted 28 March 2016
DOI: 10.1002/app.43701

INTRODUCTION

Microfluidic techniques are utilized as a versatile tool for fabricating microspheres and fibers used in a wide range of applications in drug delivery,[1,2] tissue engineering,[3–5] cosmetic and food additives,[6,7] and bioreactors.[8] T-junction,[9] co-flow,[10] and flow-focusing[11,12] methods are most commonly adopted to create mono-dispersal microsphere droplets while controlling size. Among these techniques, the flow-focusing method has advantages over other systems, such as the ability to create a smaller size of droplets and the simple fabrication steps.[13–16]

Among numerous applications, flow-focusing devices particularly in tissue engineering are used to fabricate droplets of a biocompatible prepolymer solution (hydrogel) for encapsulating cells and drugs. Researches employed flow-focusing devices to generate droplets of several types of hydrogels including magnetic hydrogel particles,[17] phenyl boronic acid groups (PMBV) and poly(vinyl alcohol) (PVA),[18] poly (ethylene glycol) (PEG),[19] gelatin methacrylate (GelMA),[20] and grapheme oxide GelMA.[21] The size and type of hydrogel droplets define the cellular microenvironment of the encapsulated cells.[18] Therefore, controlling the size of the generated droplets in microfluidic flow-focusing devices is very important for tissue engineering applications.

In a microfluidic flow-focusing devices,[11] two immiscible fluid phases (dispersed phase and continuous phase) flow into a cross-junction channel from different inlets, which results in three possible scenarios: (1) droplets are created in the orifice channel at a size bigger than the width of channel (squeezing regime); (2) droplets from the dispersed phase that are smaller than the channel are formed at the junction (dripping regime); (3) a thin stream of the dispersed phase is surrounded by the continuous phase (jetting regime).

Several experimental and numerical studies investigated the effect of different parameters on droplet generation regimes in flow-focusing devices, which include the effect of the viscosity of the two phases,[22,23] surface tension on droplet generation,[24–26] the shape of the microfluidic channel,[27,28] and the different methodologies in feeding the inflow.[29] In addition to experimental research, theoretical and computational studies

were conducted to explain the dynamics of the flow-focusing process. Particularly, researchers numerically investigated the effect of various parameters including capillary number, viscosity, and geometry on droplet generation and droplet size.[30–33] Most of these studies have investigated the droplet formation and breakup of aqueous solutions in oil. However, the fluid dynamics of biocompatible prepolymer solution is different from water, which makes optimized water-oil parameters less useful in manipulating hydrogel droplet generation.

Viscosity and surface tension are among the most important parameters influencing droplet generation regime. With the emergence of new biomaterials and hyrdogels, the range of viscosity and surface tension values in microfluidic flow-focuisng devices have been extended. Therefore, it is important to characterize the droplet formation and breakup regimes in microfluidic flow focusing systems for a wider range of viscosity, surface tension and capillary numbers which have not been studied for aquoeous solutions.

Among all biocompatible hydrogels, GelMA is one of the most popular hydrogels used in tissue engineering due to its biocompatibility,[34] mechanical properties, maintaining cell viability, and outstanding capacity for cell spreading.[35,36] To achevie the required integrity inside the cell encapsualted spheres, high concentration (and therefore high viscosity) of GelMA must be used. As a result, to achieve the capillary numbers that are required for continuous droplet genereation (dripping) regime, higher velocity of GelMA solution is needed. However, as it is shown in this study, the range of the capillary numbers that lead to dripping regime for aquoeous solutions may result in jetting regime for GelMA. As a result, to achieve dripping regime and avoid jetting regime for GelMA, lower capillary numbers (compared to that of aquoeous solutions) must be used.

In this article, to achieve a wider range of capillary numbers, we quantitatively studied the GelMA droplet generation mechanism in the flow-focusing device using both 3D computation simulations and experiments. We investigated the effects of viscosity, inertia force, and surface tension force on generating GelMA droplets. The physics of different regimes was first studied by a set of 3D computational simulation. Subsequently, we experimentally studied the effects of several key parameters, including the concentration of hydrogel, the concentration of surfactant, and the viscosity of continuous and dispersed phases. All experimental data was summarized by capillary numbers of the dispersed phase and the continuous phase to characterize the different regimes of droplet generation and to predict the transition of GelMA drops to jet. Taken together, by controlling those parameters, we can control the GelMA droplet size between 30 μm and 200 μm and achieve uniform droplet size, which will be useful for future studies in cell-laden GelMA microgels and its applications.

EXPERIMENTAL

Fabrication of Microfluidic Flow-Focusing Device

The microfluidic flow-focusing device was fabricated by the standard replica molding soft-lithography technique.[37] As shown in Figure 1(a), a thick photoresist (SU8-1025, Microchem, MA, USA) layer was coated on a silicon wafer at 500 rpm for 10 s and 2500 rpm for 30 s to create a mold. The wafer was baked at 65 °C for 5 min and at 95 °C for 10 min, and exposed to UV light through a mask for 50 seconds with the intensity at 11 mW/cm^2. A post exposure bake took place directly after exposure for 10 min at 95 °C. Finally, the substrate was immersed in a developer to remove unexposed areas of photoresist. 10:1 ratio PDMS (SYLGARD 184, Dow Corning Corporation, Midland, MI, USA) was poured over the molds in a petri dish. The device was casted and peeled off the mold. The casted PDMS flow-focusing device was bonded to the glass slide using a hand-held plasma device (BD-20, Electro-Technic Products, Chicago, IL, USA) for 1 min (at 30 s/cm^2). Figure 1(b) shows the fabricated device.

Synthesis of GelMA

GelMA was synthesized by the method described by Cha et al.[38] Briefly, 5 g of gelatin were dissolved in 45 mL of dimethyl sulfoxide at 50 °C, followed by dissolving 0.5 g of 4-(dimethylamino)-pyridine in the solution. Then, 0.5 g of glycidyl methacrylate were slowly added to the solution while it was stirring at 50 °C. The reaction was kept at 50 °C for 48 h. After synthesizing process, the solution was dialyzed against deionized (DI) water using a dialysis membrane tube (molecular weight cut off: 12000–14000 Da; Fisher Scientific, Waltham, MA, USA) for 5 days, while the deionized water was changed twice a day. Finally, the dried GelMA was made through the lyophilization process. Unless stated otherwise, all materials were purchased from Sigma-Aldrich, St. Louis, MO, USA.

Experimental Procedure

As shown in Figure 1(c), the flow-focusing device consists of two inlets, one outlet, a junction, an orifice channel, and an expanding chamber. The dispersed phase fluid is injected into the main inlet while continuous phase fluid is injected into the other inlet through syringes connected by plastic tubes (0.38 mm inner and 0.79 mm outer diameters). Continuous phase fluid flowing from two opposite sides of the channel brakes the dispersed phase at the junction, which lead to generating droplets at the junction, the orifice channel, or the expanding chamber. The flow rates of both fluids are controlled by syringe pumps (KD Scientific Inc., Holliston, MA, USA). In all experiments, the flow rate of the dispersed phase (GelMA) was kept constant at 2 μL/min, and the flow rate of continuous phase was in the range of 5–40 μL/min. For all experiments and the reliability of the results of each test, the device is continuously operated for 5 min with constant flow rate, and then the results of the experiments are recorded. The experiments are monitored by an inverted microscope.

The experiments were carried out using materials with various viscosities, densities, and surfactant concentrations for the continuous and dispersed phases. Two different concentrations of GelMA prepolymer solutions for the dispersed phase were prepared by dissolving 5 wt % and 8 wt % of GelMA in Phosphate Buffered Saline (PBS). Light mineral oil (high viscous material) and hexadecane (low viscous material, Sigma-Aldrich, St. Louis, MO, USA) with different concentrations, 0 wt %, 3 wt %, and 20 wt % of surfactant (Span 80, Sigma-Aldrich, St. Louis, MO, USA) were used for the continuous phase.

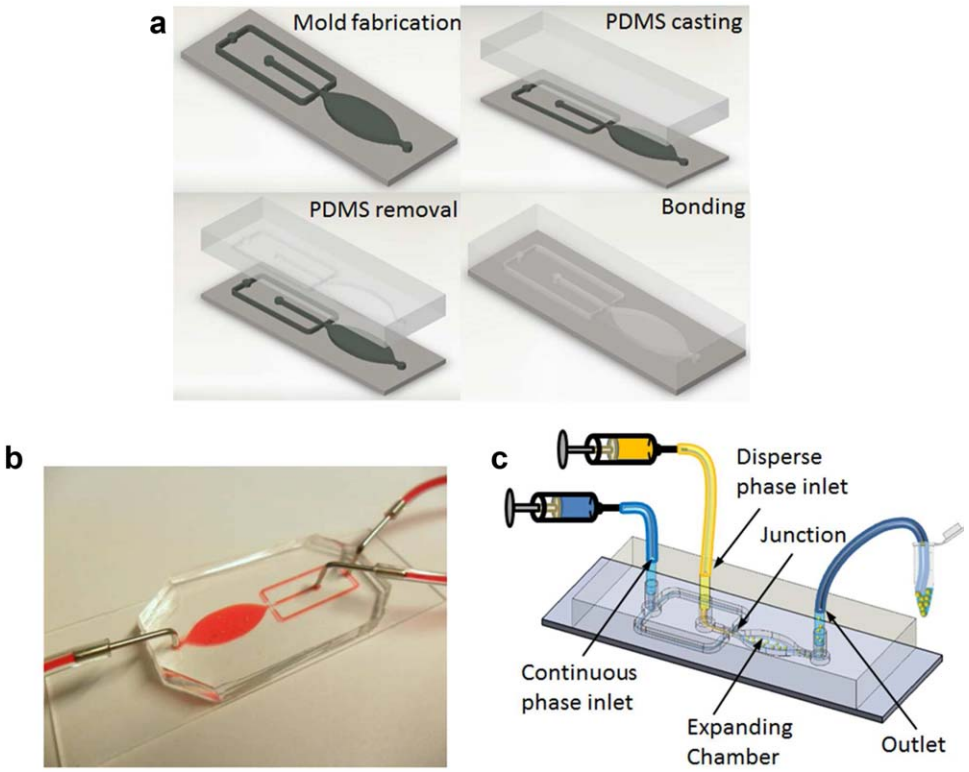

Figure 1. Design and fabrication of a flow-focusing device. (a) Replica molding microfabrication process. (b) Picture of the fabricated device bonded with a 25 mm by 75 mm glass slide. (c) Schematic of droplet generation in a flow-focusing device. [Color figure can be viewed in the online issue, which is available at wileyonlinelibrary.com.]

Computational Simulation

In this study, "Two-phase Flow, Level Set" module in COMSOL Multiphysics 4.3b (Comsol Inc., Burlington, MA, USA) was used to study the mechanism of hydrogel droplet formation in the flow-focusing device. The simulations were carried out in 3D to realistically consider the effect of all constraints. As shown in Figure 2(a), the dispersed phase (hydrogel prepolymer solution) was entered into the center inlet, while continuous phase fluid (mineral oil or hexadecane) was entered into the side inlets to meet the dispersed phase fluid at the junction. Wetted wall with $\pi/4$ constant contact angel was used as the boundary condition of the orifice channel. The geometrical dimension of 3D modeling is shown in Figure 2(a). The viscosity and density of all solutions were measured and written in Table I.

Parameters for Droplet formation

The generation of droplets and the size of droplets depend on a variety of parameters, such as the flow rate of the dispersed and continuous phases, the fluid properties of the dispersed and continuous phase, and the geometry of the device. These parameters can be summarized into two nondimensional numbers, which are called capillary number and Webber number. These two numbers govern the formation of droplets in flow-focusing devices. The capillary number describes the relationship between the viscous force and interfacial force[39] as follows,

$$Ca = \frac{\mu U}{\sigma},$$

where μ and U represent the viscosity and velocity of fluids, respectively, and σ represents the interfacial tension between the two immiscible fluids. Whereas, Webber number describes the relationship between the inertia force and interfacial force[39] as follows,

$$We = \frac{\rho U^2 D}{\sigma},$$

where ρ, U, and D represent the density, velocity of dispersed phase fluid, and channel hydraulic diameter, respectively, and σ represents the interfacial tension between the two immiscible fluids. Since the surface tension force is dominant in the low flow rate of the dispersed phase ($We \ll 1$) and the inertia force does not affect the formation of droplets,[40] we focused only on capillary numbers of the dispersed and continuous phases in this article.

RESULTS AND DISCUSSION

Computational Simulation Results

3D Computational simulations were conducted with the same geometry and fluid properties of the fabricated flow-focusing devices. In order to validate the computational results with experimental results, we compared the droplet size generated in both the simulation and experiment with the same parameters. Figure 2(b) shows the comparison of experimental and numerical results of the change in the droplet size of 5 wt % GelMA versus the various flow rate of oil with 3 wt % surfactant and Figure 2(c) shows the results of 8 wt % GelMA. As shown in these figures, the droplet size of the simulation results matches

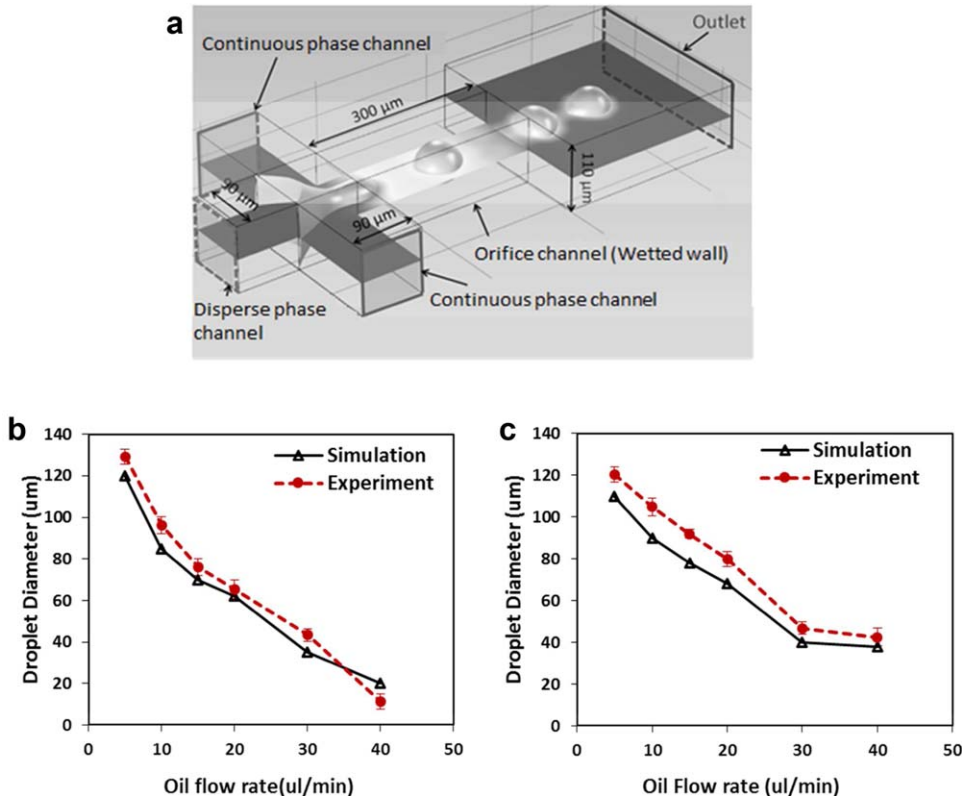

Figure 2. Detail of computational domain used for numerical simulation and validation of the proposed model with experimental results are presented. (a) Boundary condition and geometry of the flow-focusing device used in computational simulation. (b) Diameter of GelMA microgels (5 wt %) under the various flow rates of continuous fluid, mineral oil with 3 wt % surfactant (Span 80). (c) Diameter of GelMA microgels (8 wt %) under the various flow rates of continuous fluid, mineral oil with 3 wt % surfactant (Span 80). Flow rate of the disperse phase (GelMA) was 2 μL/min. For the experimental data, $n = 5$ droplets and error bar ± standard deviation for each condition. [Color figure can be viewed in the online issue, which is available at wileyonlinelibrary.com.]

well with the droplet size of the experimental results (within 10% confidence interval). The droplet size was decreased by increasing the flow rate of the continuous phase. The droplet size of 8 wt % GelMA, which was highly viscous, was not decreased anymore at a flow rate greater than 30 μL/min [Figure 2(b)]. The minimum size of 8 wt % GelMA could be achieved around 40 μm when the flow rate of the dispersal phase was 2 μL/min.

Droplet Formation Mechanism

Three different regimes: squeezing, dripping, and jetting occurred during droplet generation in the flow-focusing devices.[39] Figure 3

Table I. Fluid Properties of Mineral Oil, Hexadecane, and GelMA

	Density (kg/m^3)	Viscosity (mPa s)	Interfacial tension between oil and GelMA at 20 °C (mJ/m^2)
GelMA 5% wt	1300	2.8	
GelMA 8% wt	1500	4.9	
Mineral oil	870	27	50
Mineral oil + 3% surfactant	890	30	5
Mineral oil + 20% surfactant	1120	57.7	5
Hexadecane	780	3.3	50
Hexadecane + 3% surfactant	1020	4.2	5
Hexadecane + 20% surfactant	1080	6.7	5

Viscosity and density of each case were measured at room temperature. The interfacial tension for mineral oil-GelMA in the concentration range of 0–3% surfactant (span 80) is 50–5 mJ/m^2.[44] Since more than 3% surfactant does not change the interfacial tension, the interfacial tension for mineral oil-GelMA with the 20% surfactant is approximately 5 mJ/m^2. The interfacial tension for hexadecane-GelMA in the concentration range of 0–3% surfactant (span 80) is 50–5 mJ/m^2.[45] Since more than 3% surfactant does not change the interfacial tension, the interfacial tension for hexadecane-GelMA with 20% surfactant is approximately 5 mJ/m^2.

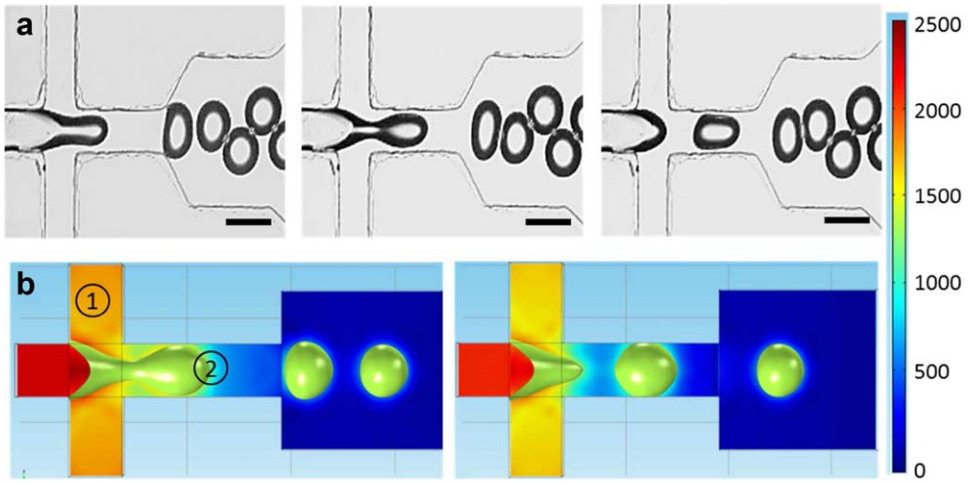

Figure 3. Droplet generation during the squeezing regime. (a) Three representative snapshots were taken the experiments. 5 wt % GelMA was used for the dispersed phase and oil with 3 wt % surfactant (span 80) was used for the continuous phase. The flow rate of the dispersed phase (Q_d) and the flow rate of continuous phase (Q_c) was 2 μL/min and 5 μL/min, respectively. Scale bar = 100 μm. (b) Numerical results of droplet generation during the squeezing regime in flow-focusing device. The flow rate of the dispersed phase (Q_d) and continuous phase (Q_c) was same as experiments. [Color figure can be viewed in the online issue, which is available at wileyonlinelibrary.com.]

shows snapshots of the droplet generation from experiments under the three regimes. In the squeezing regime, droplets were generated in the orifice channel [Figure 3(a)]. This regime occurred when the flow rate and viscosity of fluids were low. In this regime, the dispersed phase flow (GelMA) enters into the orifice and block the channel, resulting in an increase of the upstream hydrostatic pressure [pressure at point 1 in Figure 3(b)] in order to sustain the constant flow rate. The diameter of the droplet, in this case, was greater than the diameter of the orifice channel. Figure 3(b) shows the computationally simulated result of the squeezing regime. The simulation was conducted to visualize the physics of droplet generation during squeezing. The pressure change, in color, is shown in Figure 3(b). It was found that during the squeezing regime, when the dispersed phase blocked the channel, the pressure at point 1 built up to 2 kPa. When the dispersed phase blocks the channel in the squeezing regime, the difference between before [point 1 in Figure 3(b)] and after [point 2 in Figure 3(b)] the cross-junction pressure was around 0.8 kPa. Thus, the droplets break up in the squeezing regime because of the pressure build-up at the cross-junction. Garstecki et al. investigated the mechanism governing the squeezing regime in a flow-focusing device when the disperse phase is a gas.[41,42] Gas droplets were generated in a flow-focusing device at low flow rates which matches well with the results of generating hydrogel droplets at low flow rates. Both studies demonstrated that droplets can be generated at low flow rates under the squeezing regime.

During the dripping regime (shown in Figure 4) the viscosity of the continuous phase was much greater than the dispersed phase. In this case, droplets broke because of Rayleigh-Plateau instability.[43] In fact, the dispersed phase fluids tended to minimize its surface tension energy by forming a spherical shape. Therefore, the neck was formed by the continuous phase fluid, which dragged the dispersed phase fluid to the orifice channel. When the viscosity of the continuous phase fluid overcame the interfacial force of the disperse phase, the droples were cut off [Figure 4(a)]. The droplets were smaller than the width of the orifice channel. Figure 4(b) shows the computationally simulated results of the dripping regime. In the dripping regime, the pressure does not change much before or after droplet generation. The difference between before [point 1 in Figure 4(b)] and after [point 2 in Figure 4(b)] the cross-junction pressure is around 0.4 kPa, which is smaller than the squeezing regime (0.8 kPa), and droplets breakup in this regime because of the Rayleigh-Plateau instability theory.

In the jetting regime (shown in Figure 5), the thin stream of the dispersed phase was created and droplets were finally cut off in the expansion chamber as a result of Rayleigh-Plateau instability. This regime occurred when the viscosity of the continuous and dispersed phases were both high. The viscosity of the continuous phase dragged the dispersed phase, but the formation of the droplets were suppressed because of the high viscousity of the dispersed phase, resulting during the jetting regime.

Various Parameters for Controlling Droplet Size

In order to study the effect of surface tension on droplet generation, hexadecane, and mineral oil without surfactant were compared with hexadecane and mineral oil with 3% surfactant (Span 80). By adding surfactant up to 3% to the fluid, the surface tension of the continuous phase liquids was dramatically decreased. However, it did not change the viscosity of the liquids. The values of surface tension for each case are shown in Table I.

The diameters of the droplets created by mineral oil and hexadecane, with different percentage of surfactant, are shown in Figure 6. Comparing the results of hexadecane without surfactant, hexadecane with 3% surfactant, mineral oil without surfactant, and mineral oil with 3% surfactant shows that when surface tension between two immiscible fluid drops, the size of droplets were decreased. In addition to the effect of surfactant

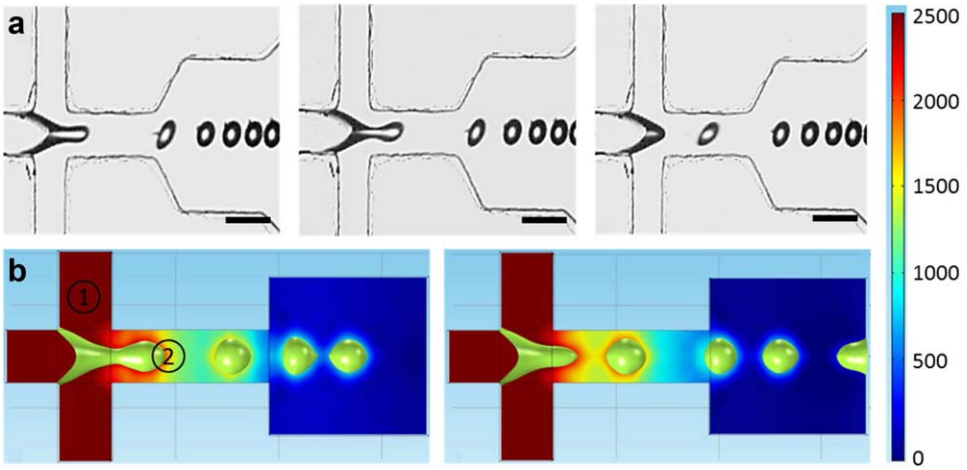

Figure 4. Droplet generation during the dripping regime. (a) Three representative snapshots were taken the experiments. 5 wt % GelMA was used for the dispersed phase and oil with 3 wt % surfactant (span 80) was used for the continuous phase. The flow rate of the dispersed phase (Q_d) and the flow rate of continuous phase (Q_c) was 2 μL/min and 20 μL/min, respectively. Scale bar = 100 μm. (b) Numerical results of droplet generation during the dripping regime in flow-focusing device. The flow rate of the dispersal phase (Q_d) and flow rate of the continuous phase (Q_c) was same as experiments [Color figure can be viewed in the online issue, which is available at wileyonlinelibrary.com.]

on decreasing the size of droplets, uniform monodisperse droplets were created by adding the surfactant to the continuous phase. The polydispersity index, defined as the ratio between the standard deviation and the mean diameter of particles multiplied by 100, for all the cases were calculated and summarized in Table II. Droplets that were created without the surfactant easily merged after generation, resulting in nonuniform droplet sizes [Figure 7(a)].

In order to study the effect of the dispersed phase viscosity (GelMA concentration), two different solutions of GelMA 5 wt % [Figure 6(a,c)] and 8 wt % [Figure 6(b,d)] were carried out. It was found that the generated droplet diameters were very sensitive to the concentration of GelMA. Comparing the cases with the same continuous phase, but different GelMA concentration (as their dispersed phase), it was found that droplet size increases by increasing the GelMA concentration. This suggests that the size of the droplet does not only depend on the viscosity of a continuous phase, but also depends on GelMA concentration. In addition, the jetting regime observed, when GelMA 8 wt % and mineral oil with 20 wt % surfactant (for the dispersed phase and the continuous phase, respectively) were used, due to the high viscosity of the continuous phase fluid and dispersed phase fluid [Figure 6(d)]. Using a higher concentration of GelMA makes the inertia force of the dispersed phase to be considerable, which results in creating a jetting regime. In this study the flow rate of hydrogel prepolymer solution kept constant at 2 μL/min in order to prevent the formation of jetting regime. At higher flow rate of hydrogel prepolymer solution, the inertia force of dispersed phase fluid (hydrogel prepolymer solution) becomes dominate and the Webber number of disperse phase is more than (We >1), resulting in a stream of jet.

The effect of viscosity of the continuous phase was studied by comparing cases of mineral oil and hexadecane with 3% surfactant (μ = 4.2 mPa·s) and 20% surfactant (μ = 6.7 mPa·s). Adding more than 3% surfactant to the fluid will not change the interfacial tension between the dispersed phase fluid and the continuous phase fluid because of Micelle effect.[46] However, it increases the viscosity of the fluids dramatically. Figure 6(a,b) show droplet sizes when hexadecane was used as a continuous phase. Comparing hexadecane with 3% surfactant and 20% surfactant shows that the size of the droplets was decreased by increasing the viscosity of the continuous phase (the amount of surfactant). Also, the same results are shown by comparing the mineral oil and hexadecane (Figure 6), since the viscosity of

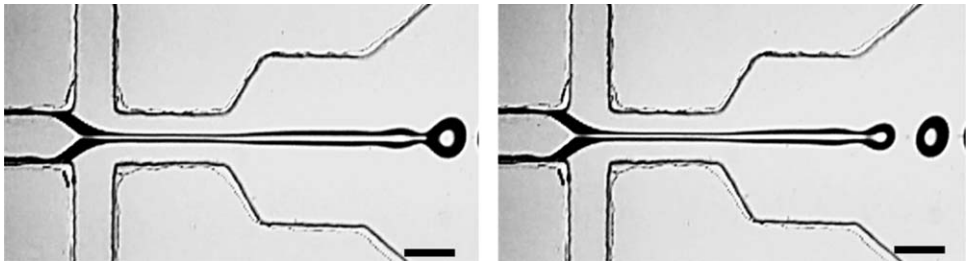

Figure 5. Two snapshots of droplet generation during the jetting regime. 8 wt % GelMA was used for the dispersed phase and oil with 20 wt % surfactant (span 80) was used for the continuous phase. The flow rate of the dispersed phase (Q_d) and flow rate of the continuous phase (Q_c) was 2 μL/min and 40 μL/min, respectively. Scale bar = 100 μm.

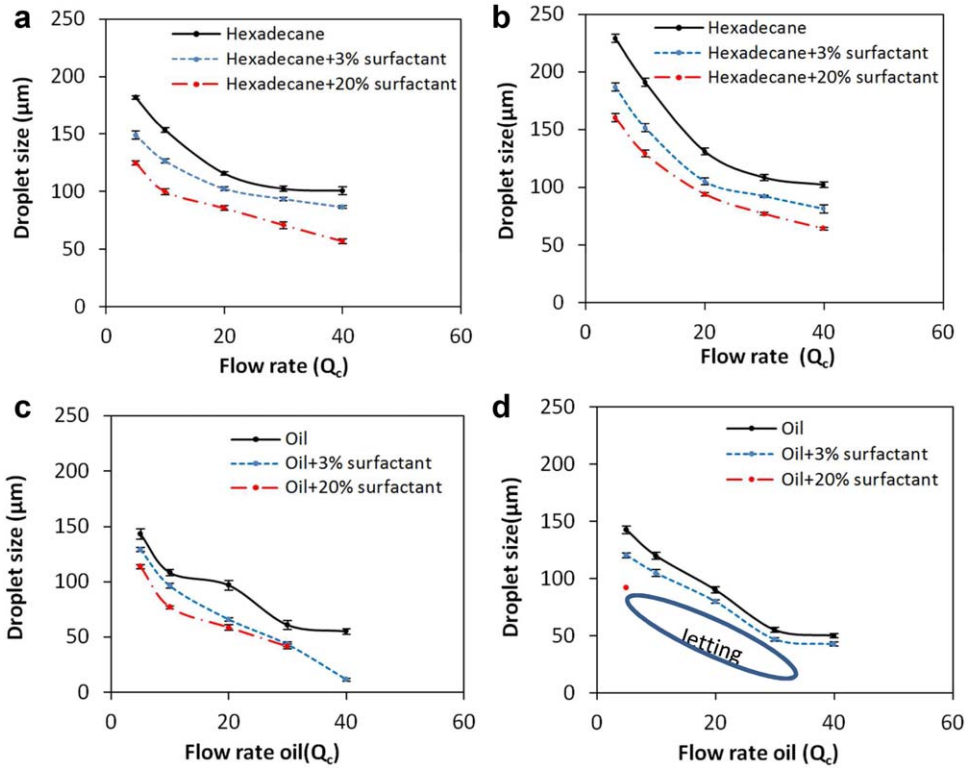

Figure 6. GelMA droplet sizes versus various flow rate of oil. (a) 5 wt % GelMA was used for the dispersed phase, and Hexadecane with different concentration of surfactant, 0 wt %, 3 wt %, and 20 wt %, was used for the continuous phase. (b) 8 wt % GelMA was used for the dispersed phase, and Hexadecane with different concentration of surfactant, 0 wt %, 3 wt %, and 20 wt %, was used for the continuous phase. (c) 5 wt % GelMA was used for the dispersed phase, and mineral oil with different concentration of surfactant, 0 wt %, 3 wt %, and 20 wt %, was used for the continuous phase. (d) 8 wt % GelMA was used for the dispersed phase, and mineral oil with different concentration of surfactant, 0 wt %, 3 wt %, and 20 wt %, was used for the continuous phase. The flow rate of the dispersed phase was kept constant in all cases at 2 µL/min. The flow rate of the continuous phase was changed in range of 5 µL/min–10µL/min. The number of measurement for droplet size is five and standard deviation is shown for five droplets in each cases. [Color figure can be viewed in the online issue, which is available at wileyonlinelibrary.com.]

hexadecane is much less than mineral oil while the surface tension of mineral oil and hexadecane is almost the same. In addition, the high viscosity of the continuous phase fluid caused the dispersed phase fluid to stretch into long thin streams. At high viscosity of continuous phase, it is difficult to fabricate 8 wt % GelMA. However, higher concentration of GelMA is required for fabricating stiffer microgels in some applications. In addition, UV exposure time to crosslink the hydrogel is decreased with higher concentration of GelMA, resulting in higher cell viability for cell-laden hydrogel application. According to Figure 6, small 8 wt % GelMA droplets could be created when less viscous continuous phase fluid (e.g., hexadecane) was used. When hexadecane used as a continuous phase, due to the low viscosity of the hexadecane, GelMA droplets of two different concentrations (5 wt % and 8 wt %) were created through the squeezing regime. These results show that hexadecane could be a good

Table II. The Polydispersity Index Was Summarized for All the Cases

Fluids conditions	5 µL/min	10 µL/min	20 µL/min	30 µL/min	40 µL/min
5 wt % GelMA and Mineral oil with 3 wt % surfactant	3.2%	4.6%	4.5%	9.6%	2.3%
5 wt % GelMA and Mineral oil with 20 wt % surfactant	3%	2.8%	8%	10%	Jetting
8 wt % GelMA and Mineral oil with 3 wt % surfactant	3.5%	5.2%	3.2%	6%	8%
5 wt % GelMA and Hexadecane with 3 wt % surfactant	3.8%	2.3%	3.2%	2.9%	2.6%
5 wt % GelMA and Hexadecane with 20 wt % surfactant	2.4%	4%	3.4%	7.1%	12.7%
8 wt % GelMA and Hexadecane with 3 wt % surfactant	2.4%	2.9%	3.45	3.9%	8.3%
8 wt % GelMA and Hexadecane with 20 wt % surfactant	4.5%	4.5%	3.1%	3.6%	4.2%

Two different concentrations (i.e., 5 and 8 wt %) of GelMA as the dispersed phase was used. Two different oils (i.e., Mineral oil and hexadecane) with various amounts of surfactant (span 80) were used as the continuous phase. The flow rate of dispersed phase was constant (2 µL/min) for all the experiments while the flow rates of continuous phase were between 5 µL/min and 40 µL/min.

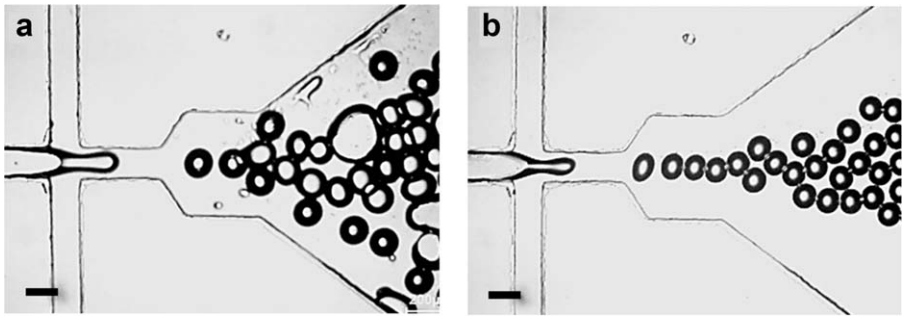

Figure 7. Effect of surfactant on the droplet generation. 5 wt % GelMA was used for the dispersed phase with two different solution for the continuous phase: (a) mineral oil without surfactant (b) mineral oil with 3 wt % surfactant. Flow rate of GelMA and flow rate of the continuous phase was 2 μL/min and 10 μL/min, respectively. Scale bar = 100 μm.

option for fabricating high concentration of hydrogel droplets in tissue engineering application. Moreover, hexadecane presents high biocompatibility using as a continuous phase for fabricating cell-laden alginate droplets.[47]

Figure 8 shows the effect of the flow rate for the continuous phase. The sizes of the droplets were dramatically decreased by increasing the flow rate of a continuous phase. By increasing the flow rate of the continuous phase, the viscosity of the continuous phase increased, thus, the high viscosity of the continuous phase suppressed the dispersed phase fluid, resulting in the small size of droplets.

Characterization of Hydrogel Droplet Generation Regime

Figure 9 shows a phase diagram of GelMA droplet generation observed through the experiments. Capillary numbers of each experiment were calculated and plotted in Figure 9 to predict the formation of GelMA droplets or a jet stream in a flow-focusing device. In flow-focusing geometry, nondimensional capillary numbers are important in describing the transition between the dripping and the jetting regime, because the viscosity of the continuous phase and the interfacial force are more important than the inertia force in flow-focusing devices. The capillary number of the continuous phase $Ca_c = \mu v/\sigma$ and disperse phase $Ca_d = \mu v/\sigma$ described in Figure 9 shows the range of formation of each regime. The result show that at very low capillary numbers of continuous ($Ca_c < 10^{-2}$) and dispersed phase fluids ($Ca_d < 10^{-2}$), the squeezing regime happens and droplets are created at a size bigger than the width of the channel. When $10^{-2} < Ca_c < 10^{-1}$ and $Ca_d < 10^{-2}$, the dripping regime happens and the droplets are created at a size smaller

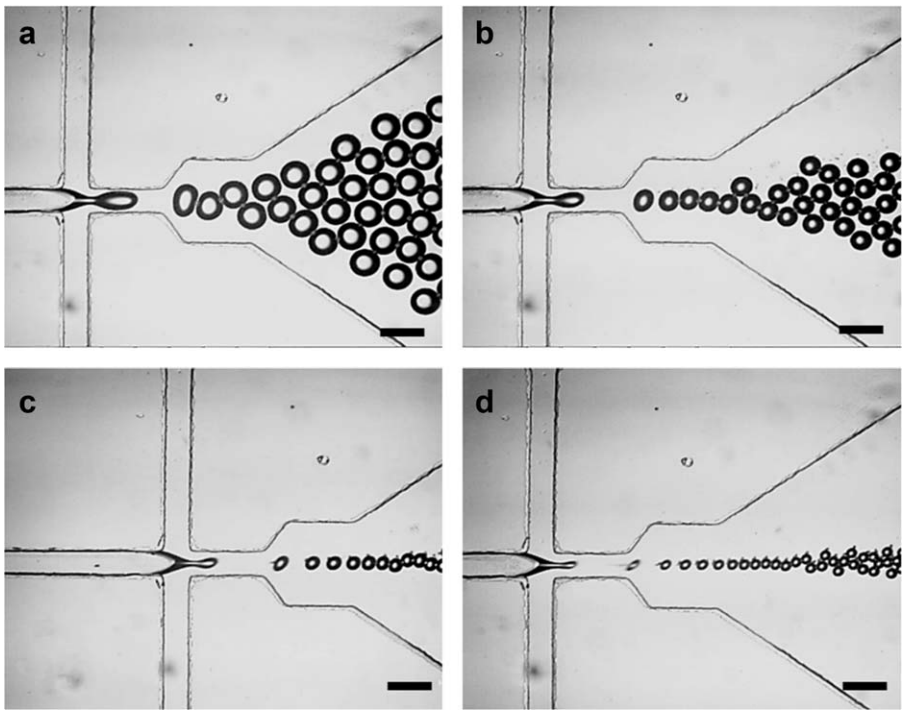

Figure 8. GelMA microgels generation in flow-focusing device under various flow rate of the continuous phase, (a) $Q_c = 5$ μL/min, (b) $Q_c = 10$ μL/min, (c) $Q_c = 20$ μL/min, and (d) $Q_c = 30$ μL/min. 5 wt % GelMA was used for the dispersed phase and mineral oil with 3 wt % surfactant (Span 80) was used for the continuous phase. Flow rate of dispersed phase was $Q_d = 2$ μL/min. Scale bar = 200 μm.

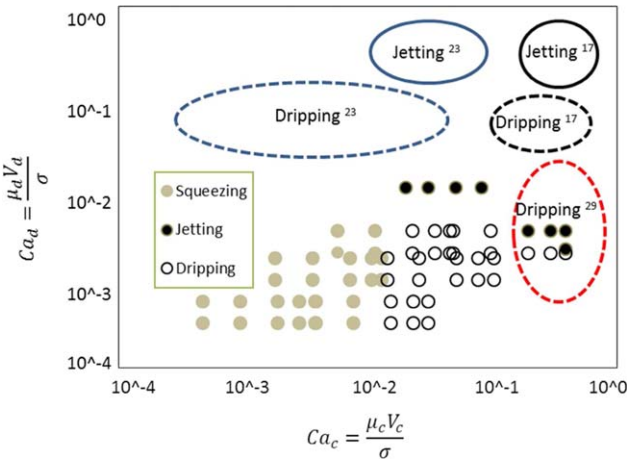

Figure 9. Diagram shows three different regimes resulting from the flow-focusing device in comparison with previously reported results [Color figure can be viewed in the online issue, which is available at wileyonlinelibrary.com.]

than the width of the channel. At high capillary numbers of continuous phase fluid ($10^{-1} < Ca_c < 10$) and $Ca_d < 10^{-2}$, the thin jet stream of the dispersed phase fluid is created. The results show that the transition from dripping regime to the jetting regime happens at $Ca_c \sim 10^{-1}$. This phase diagram provides a comprehensive study of hydrogel droplet generation in tissue engineering application. The capillary numbers of jetting and dripping regime observed from different studies[23,39] is also shown in the phase diagram. According to the results,[39] most of capillary numbers of aqueous phase observed in their experiments were in range of $Ca_d > 10^{-2}$. However, due to the viscosity of hydrogels (the viscosity of 5 wt % GelMA is 2.8 mPa·s and 8 wt % GelMA 4.9 mPa·s), GelMA prepolymer droplets cannot be created in even relatively low capillary number of the dispersed phase ($Ca_d \sim 10^{-2}$). Therefore, the results from the previous studies for droplet generation of water in oil are not applicable for hydrogel droplet generation for tissue engineering application. This phase diagram provides a comprehensive study of hydrogel droplet generation in tissue engineering application.

CONCLUSIONS

In this article, we discussed the effect of fluid properties, including viscosity, density, and surface tension as well as the flow rate of the dispersed phase for hydrogel droplet generation in the flow-focusing devices. GelMA prepolymer solution with two different concentrations, 5 wt %, and 8 wt %, were used for the dispersed phase. Two different oils, hexadecane, and light mineral oil, with different concentration of surfactant, 0 wt %, 5 wt %, and 20 wt %, were used for the continuous phase. Experiments were carried out using different flow rates of continuous phase to study the influence of effective forces on droplet generation. Three different regimes (squeezing, dripping, and jetting) were investigated via simulation and characterized by experiments. All the results were summarized in two none dimensional numbers, Ca_c and Ca_d, to determine the range of the squeezing, dripping, and jetting regimes. It was found that the concentration of GelMA dramatically affected the creation of droplets during the jetting regime. The results show that the size of the droplets created using mineral oil at a continuous phase are much smaller than those created using hexadecane at a continuous phase, because of the higher viscosity of the mineral oil. By controlling the flow rate of the two phases, the type of oil, and the concentration of surfactant, the droplet size of the phase with different GelMA concentrations can be manipulated between 30 μm and 250 μm, which will be very useful to further control the number of encapsulated cells and their nearby microenvironment.

ACKNOWLEDGMENTS

This work was supported by Natural Sciences and Engineering Research Council of Canada Discovery Grant (RGPIN-2014-04010).

REFERENCES

1. Xu, Q.; Hashimoto, M.; Dang, T. T.; Hoare, T.; Kohane, D. S.; Whitesides, G. M.; Langer, R.; Anderson, D. G.; David, H. *Small* **2009**, *5*, 1575.
2. Dai, R.; Wang, Z.; Samanipour, R.; Koo, K.; Kim, K. *Stem Cells Int.* **2016**, *2016*, 6737345.
3. Chung, B. G.; Lee, K. H.; Khademhosseini, A.; Lee, S. H. *Lab Chip* **2012**, *12*, 45.
4. Wang, Z.; Samanipour, R.; Koo, K.; Kim, K. *Sens. Mater.* **2015**, *27*, 487.
5. Wang, Z.; Samanipour, R.; Kim, K. In Biomedical Engineering: Frontier Research and Converging Technologies; Jo, H., Jun, H.-W., Shin, J., Lee, S.-H., Eds.; Springer: Switzerland, **2016**; pp 209–233.
6. Desai, K. G. H.; Park, J. H. Dry. Technol. 2005, 23, 1361.
7. Gouin, S. *Trends Food Sci. Technol.* **2004**, *15*, 330.
8. Retterer, S. T.; Siuti, P.; Choi, C. K.; Thomas, D. K.; Doktycz, M. J. *Lab Chip* **2010**, *10*, 1174.
9. Nisisako, T.; Torii, T.; Higuchi, T. *Lab Chip* **2002**, *2*, 24.
10. Utada, A. S.; Fernandez-Nieves, A.; Stone, H. A.; Weitz, D. A. *Phys. Rev. Lett.* **2007**, *99*, 1.
11. Anna, S. L.; Bontoux, N.; Stone, H. A. *Appl. Phys. Lett.* **2003**, *82*, 364.
12. Parker, B.; Samanipour, R.; Ahmadi, A.; Kim, K. **2015**, *11*, 41.
13. Cygan, Z. T.; Cabral, J. T.; Beers, K. L.; Amis, E. J. *Langmuir* **2005**, *21*, 3629.
14. Jahn, A.; Reiner, J. E.; Vreeland, W. N.; DeVoe, D. L.; Locascio, L. E.; Gaitan, M. *J. Nanopart. Res.* **2008**, *10*, 925.
15. Dendukuri, D.; Doyle, P. S. *Adv. Mater.* **2009**, *21*, 4071.
16. Wang, H.; Zhang, W.; Dai, Z. *Anal. Methods.* **2014**, *6*, 9754.
17. Chen, C. H.; Abate, A. R.; Lee, D.; Terentjev, E. M.; Weitz, D. A. *Adv. Mater.* **2009**, *21*, 3201.
18. Aikawa, T.; Konno, T.; Takai, M.; Ishihara, K. *Langmuir* **2012**, *28*, 2145.
19. Dang, T. D.; Kim, Y. H.; Kim, H. G.; Kim, G. M. *J. Ind. Eng. Chem.* **2012**, *18*, 1308.

20. Jung, J.; Oh, J. *Biomicrofluidics* **2014**, *8*, 036503.
21. Shin, S. R.; Aghaei-Ghareh-Bolagh, B.; Dang, T. T.; Topkaya, S. N.; Gao, X.; Yang, S. Y.; Jung, S. M.; Oh, J. H.; Dokmeci, M. R.; Tang, X.; Khademhosseini, A. *Adv. Mater.* **2013**, *25*, 6385.
22. Nie, Z.; Seo, M.; Xu, S.; Lewis, P. C.; Mok, M.; Kumacheva, E.; Whitesides, G. M.; Garstecki, P.; Stone, H. A. *Microfluid. Nanofluidics* **2008**, *5*, 585.
23. Cubaud, T.; Mason, T. G. *Phys. Fluids* **2008**, *20*, 1.
24. Anna, S. L.; Mayer, H. C. *Phys. Fluids* **2006**, *18*, 121512.
25. Lee, W.; Walker, L. M.; Anna, S. L. *Macromol. Mater. Eng.* **2011**, *296*, 203.
26. Peng, L.; Yang, M.; Guo, S.; Liu, W.; Zhao, X. *Biomed. Microdevices* **2011**, *13*, 559.
27. Dollet, B.; Van Hoeve, W.; Raven, J. P.; Marmottant, P.; Versluis, M. *Phys. Rev. Lett.* **2008**, *100, 1*,
28. Humphry, K. J.; Ajdari, A.; Fernández-Nieves, A.; Stone, H. A.; Weitz, D. A. *Phys. Rev. E Stat. Nonlin. Soft Matter Phys.* **2009**, *79*, 1.
29. Ward, T.; Faivre, M.; Abkarian, M.; Stone, H. A. *Electrophoresis* **2005**, *26*, 3716.
30. Shi, Y.; Tang, G. H.; Xia, H. H. *Comput. Fluids* **2014**, *90*, 155.
31. Gupta, A.; Matharoo, H. S.; Makkar, D.; Kumar, R. *Comput. Fluids* **2014**, *100*, 218.
32. Lee, W.; Walker, L. M.; Anna, S. L. *Phys. Fluids* **2009**, *21*, 1.
33. Schneider, T.; Burnham, D. R.; VanOrden, J.; Chiu, D. T. *Lab Chip* **2011**, *11*, 2055.
34. Wang, Z.; Abdulla, R.; Parker, B.; Samanipour, R. *Biofabrication* **2015**, *7*, 1.
35. Nichol, J. W.; Koshy, S. T.; Bae, H.; Hwang, C. M.; Yamanlar, S.; Khademhosseini, A. *Biomaterials* **2010**, *31*, 5536.
36. Jung, J.; Oh, J. *e-Polymers* **2014**, *14*, 161.
37. Xia, Y.; Whitesides, G.M. *Annu. Rev. Mater. Sci.* **1998**, *28*, 153.
38. Cha, C.; Oh, J.; Kim, K.; Qiu, Y.; Joh, M.; Shin, S. R.; Wang, X.; Camci-Unal, G.; Wan, K. T.; Liao, R.; Khademhosseini, A. *Biomacromolecules* **2014**, *15*, 283.
39. Nunes, J. K.; Tsai, S. S. H.; Wan, J.; Stone, H. A. *J. Phys. D: Appl. Phys.* **2013**, *46*, 114002.
40. Lagus, T. P.; Edd, J. F. *J. Phys. D: Appl. Phys.* **2013**, *46*, 114005.
41. Baroud, C. N.; Gallaire, F.; Dangla, R. *Lab Chip* **2010**, *10*, 2032.
42. Garstecki, P.; Stone, H. A.; Whitesides, G. M. *Phys. Rev. Lett.* **2005**, *94*, 164501.
43. Rayleigh, L. *Proc. R. Soc. Lond.* **1879**, *29*, 71.
44. Sun, M.; Bithi, S. S.; Vanapalli, S. A. *Lab Chip* **2011**, *11*, 3949.
45. Drelich, J.; Miller, J. D. *Ann. Univ. Mariae Curie Sklodowska* **1999**, *54*, 105.
46. Phillips, B. Y. J. N. *Trans. Faraday Soc.* **1955**, *51*, 561.
47. Choi, C. H.; Jung, J. H.; Rhee, Y. W.; Kim, D. P.; Shim, S. E.; Lee, C. S. *Biomed. Microdevices* **2007**, *9*, 855.